Spatial Relationship of Biomass and Species Distribution in an Old-Growth *Pseudotsuga-Tsuga* Forest

Jiquan Chen, Bo Song, Mark Rudnicki, Melinda Moeur, Ken Bible, Malcolm North, Dave C. Shaw, Jerry F. Franklin, and Dave M. Braun

ABSTRACT. Old-growth forests are known for their complex and variable structure and function. In a 12-ha plot (300 m × 400 m) of an old-growth Douglas-fir forest within the T. T. Munger Research Natural Area in southern Washington, we mapped and recorded live/dead condition, species, and diameter at breast height to address the following objectives: (1) to quantify the contribution of overstory species to various elements of aboveground biomass (AGB), density, and basal area, (2) to detect and delineate spatial patchiness of AGB using geostatisitcs, and (3) to explore spatial relationships between AGB patch patterns and forest structure and composition. Published biometric equations for the coniferous biome of the region were applied to compute AGB and its components of each individual stem. A program was developed to randomly locate 500 circular plots within the 12-ha plot that sampled the average biomass component of interest on a per hectare basis so that the discrete point patterns of trees were statistically transformed to continuous variables. The forest structure and composition of low, mediate, and high biomass patches were then analyzed. Biomass distribution of the six major species across the stand were clearly different and scale- dependent. The average patch size of the AGB based on semivariance analysis for *Tsuga heterophylla, Abies amabilis, A. grandis, Pseudotsuga menziesii, Thuja plicata,* and *Taxus brevifolia* were 57.3, 81.7, 37, 114.6, 38.7, and 51.8 m, respectively. High biomass patches were characterized by high proportions of *T. heterophylla* and *T. plicata* depending on spatial locations across the stand. Low AGB patches had high densities of *A. amabilis* and *T. brevifolia.* We presented several potential mechanisms for relating spatial distribution of species and biomass, including competition, invasion and extinction, disturbance, and stand dynamics. Clearly, future studies should be developed to examine the details of how each process alters the spatial patterns of tree species with sound experimental designs and long-term monitoring processes at multiple scales. FOR. SCI. 50(3):364–375.

Key Words: Spatial pattern analysis, canopies, old-growth, aboveground biomass (AGB), semivariogram, Douglas-fir, WRCCRF.

J. Chen, Earth, Ecological, and Environmental Science, University of Toledo, Toledo, OH 43606—jiquan.chen@utoledo.edu. B. Song, Department of Forest Resources, Belle W. Baruch Institute of Coastal Ecology and Forest Science, Clemson University, Georgetown, SC 29442—bosong@clemson.edu. M. Rudnicki, Department of Renewable Resources, University of Alberta, Edmonton, Alberta, T6G 2E3, Canada—mark_rudnicki@hotmail.com. M. Moeur, Interagency Monitoring Program, USDA Forest Service, Portland, OR 97208—mmoeur@fs.fed.us. M. North, Sierra Nevada Research Center, Department of Environmental Horticulture, University of California, Davis, CA 95616—mpnorth@ucdavis.edu. K. Bible, D. Shaw, J. Franklin, and D. Braun, College of Forest Resources, University of Washington, Seattle, WA 98195—kbible@u.washington.edu, dshaw@u.washington.edu, jff@u.washington.edu, and dbraun@u.washington.edu.

Manuscript received March 11, 2002, accepted June 12, 2003.

A RECENT MOVEMENT IN ECOLOGICAL THEORY describes ecosystem or community characteristics as being coherently organized in space and time, and implies that this intrinsic organization controls or moderates ecosystem function (Holling 1992, Levin 1992). For example, a conceptual framework was proposed for arid ecosystems where "fertility islands" create a structuring mosaic that maintains the ecosystem's overall function and stability (Burke et al. 1999, Schlesinger et al. 1996). In forested ecosystems, ecologists have proposed a framework of gap mosaics and patch dynamics to explain the coherent relationships between spatial structure and function (Runkle 1981, Pickett and White 1985, Spies and Franklin 1989, Lieberman et al. 1989, Chen and Franklin 1997). Observational (e.g., Lertzman et al. 1996, Van Pelt and Franklin 1999), experimental (e.g., Gray and Spies 1997, Rudnicki and Chen 2000), and modeling (e.g., Botkin 1993, Song et al. 1997) studies have demonstrated that ecosystem processes such as understory development, regeneration, water translocation, tree growth and death, and nutrient cycling are spatially constrained by the structural mosaic of a forest that is made up of canopy openings, or gaps, and tree patches of differing structure. Chen and Bradshaw (1999) argued that much of forest function could not be mechanistically understood without detailed exploration of structure (including canopies) in three-dimensional space and across multiple scales.

Scale is a critical parameter in quantifying forest structure (Bradshaw and Spies 1992, Busing 1998, Song et al. 1997). At fine scales (a few meters), tree distributions may shift from clumped to regular as forest succession proceeds (Moeur 1993, Ward et al. 1996) because density-dependent mortality thins regeneration clumps and large trees are regularly spaced due to resource limitations. At a larger scale (tens of meters), stand density is clumped because productivity varies with stand heterogeneity such as topography, soil, and disturbance history (Szwagrzyk 1990, He et al. 1997, Chen and Bradshaw 1999, Van Pelt and Franklin 1999). Consequently, stem distribution and associated canopy patchiness will have direct control of the functional attributes of an ecosystem such as production. To investigate across scales, we used a 12-ha (300 × 400 m) stem map to analyze forest spatial structure from tree-to-tree interactions up to 150 m. We were also interested in whether the spatial distributions of trees, analyzed across a range of scales, had any significant effect on ecosystem productivity.

Tree distribution in a stand is a product of complex interactions among many processes including species' life histories, fine-scale environmental variation, disturbance regime, competition among individuals and populations, seed dispersal and success of regeneration, and stochastic processes such as windthrows and outbreaks of insects and diseases. Although pattern analysis of current structure alone cannot determine the particular process responsible for an observed stand structure, it can help guide inferences about potentially important community processes and assess ecosystem stability, productivity, and other functions. We hypothesized that distribution of trees (measured by species) and patchiness of biomass are spatially correlated, primarily because community composition and tree size directly determined biomass across the stand. Specifically, our objectives were to: (1) quantify the contribution of overstory species to various elements of aboveground biomass (AGB), density (D), and basal area (BA) in an old-growth Douglas-fir (*Pseudotsuga menziesii* (Mirb.) Franco) forest; (2) detect and delineate spatial patchiness of AGB using semivariance analysis and kriging; and (3) explore spatial coherencies between AGB distribution and forest structure and composition.

Methods

Study Area

Our study site is located within the T.T. Munger Research Natural Area (RNA, 45°49′ N and 121°58′ W) of the Gifford Pinchot National Forest in the Cascade Mountains of southwest Washington State. The research site is on the lower slopes of an inactive quaternary shield volcano, Trout Creek Hill, on gentle topography. The sandy, shotty loam soils developed from tephra 2–3 m deep and are classified as entic dystrandepts belonging to the Staebler series. The climate is cool and wet, with a distinct summer drought. Mean total annual precipitation is 2,528 mm, while June through Aug. precipitation is 119 mm. Mean annual temperature is 8.7° C, with a Jan. mean of 0° C, and a July mean of 17.5° C. Average annual snowfall, 233 cm, is quite variable as this site is in the lower Cascade Mountain slopes (Franklin and DeBell 1988).

The T.T. Munger RNA is the site of a long-term study established in 1947 on growth, mortality, and succession (DeBell and Franklin 1987, Franklin and DeBell 1988). Ages of the dominant pioneer *Pseudotsuga menziesii*

Acknowledgments: Funding for this project was partially provided by the USDA Forest Service Pacific Northwest Experimental Station (PNW94-0541), the Earthwatch Institute and the Durfee Foundation's Student Challenge Awards Program, the Western Regional Center for Global Environmental Change of the Department of Environment, and the Charles Bullard Fellowship of the Harvard University (to J. Chen). We thank the following individuals for their help in data collection: Meredith Alan, Joel Benjamin, Joseph Brown, Hannah Chapin, Tim Crosby, Maria Garety, Matthew Madden, Heather Michaud, Cezary Mudrewicz, Scott Ramsburg, Angelia Smith, Lucia Stoisor, Julia Svoboda, and Beata Ziolkowska. Dee Robbins contributed a significant amount of time and thought to support our Earthwatch expeditions in 1997 and 1998. We thank the Wind River Canopy Crane Research Facility, The Gifford Pinchot National Forest, and Elizabeth Freeman for installation of the four hectares surrounding the canopy crane. Hiroaki Ishii and Elizabeth Freeman also participated in early fieldwork. Sari Saunders, Eugenie Euskirchen, Kim Armington, Mary Bresee, Jeoffrey Parker, and two anonymous reviewers provided valuable suggestions to improve the manuscript.

(PSME) range from 250 to >450 years (Franklin and Waring 1980). They are slowly dying out of the stand and are being replaced by *Tsuga heterophylla* Raf., Sarg. (TSHE), *Thuja plicata* Donn (THPL), *Abies amabilis* (Dougl.) Forbes (ABAM), and *Abies grandis* (Dougl.) Lindl (AGBR). Also disappearing from the stand is *Abies procera* Rehd. (ABPR). Another pioneer species, *Pinus monticola* Dougl. Ex D. Don. (PIMO), was once more prevalent, but is disappearing due to a combination of blister rust (*Ronartium ribicola* Fischer)—an introduced fungal pathogen from Eurasia—and a native bark beetle—*Dendroctonus ponderosae* Hopkins—(Franklin and DeBell 1988). Dominant shrubs include *Acer circinatum* Pursh, *Gaultheria shallon* Pursh, *Berberis nervosa* Pursh, and *Vaccinium parvifolium* Smith. Dominant herbs, though not as abundant as shrubs, include *Achlys triphylla* (Smith) DC., *Vancouveria hexandra* (Hook.) Morr. & Dec., *Pteridium aquilinum* (L.) Kuhn, *Linnaea borealis* L., and *Xerophyllum tenax* (Pursh) Nutt. In 1995, an 85-m tall construction crane known as Wind River Canopy Crane Research Facility (WRCCRF) was installed in the western edge of the RNA for conducting ecological investigations within forest canopies.

Data Collection

A 4-ha square plot was established by a professional survey consulting firm in 1994 before the installation of the canopy crane. The plot was divided into a 25-m grid and marked with 50-cm reinforcement bars and aluminum caps. The WRCCRF researchers tagged all trees ≥5 cm in diameter at breast height (dbh: 1.37 m above the ground) with a precoded aluminum tag, tallied live/dead condition, and measured the coordinates of each tree within the plot, utilizing a Criterion 4000 survey laser station and the grid points marking the plot corners (Freeman 1997). Tree base elevations were calculated based on inclination measurements using the Criterion, and the elevations of the grid points that were measured in 1996 were determined using a total survey station (Wild TC600 total survey station). Using a similar protocol in 1996, we added another 4-ha plot adjacent to the west boundary. An additional 100 × 400-m plot (4-ha) was added along the southern border of the combined 8-ha in the summers of 1996 and 1997 for a total of 12-ha (Figure 1). After mapping all trees, we measured any cumulative surveying error by remeasuring original grid points and found <15 cm of difference on average.

Biomass Distribution and Geostatistical Analysis

Unlike tree distributions across a stand, which are discrete point patterns, spatial distribution of volume and biomass could be considered as continuous variables. Their spatial patterns can be best described using methods such as spectral (Cressie 1993) or wavelet analysis (Bradshaw and Spies 1992, Chen et al. 1999). Three steps were taken to quantitatively characterize the spatial distributions of AGB, including biomass of stem wood and bark and live branches, and foliage biomass. We applied dbh-height models (Song 1998, Ishii et al. 2000) to calculate tree height by species based on field-measured dbh. Heights of PIMO and ABPR

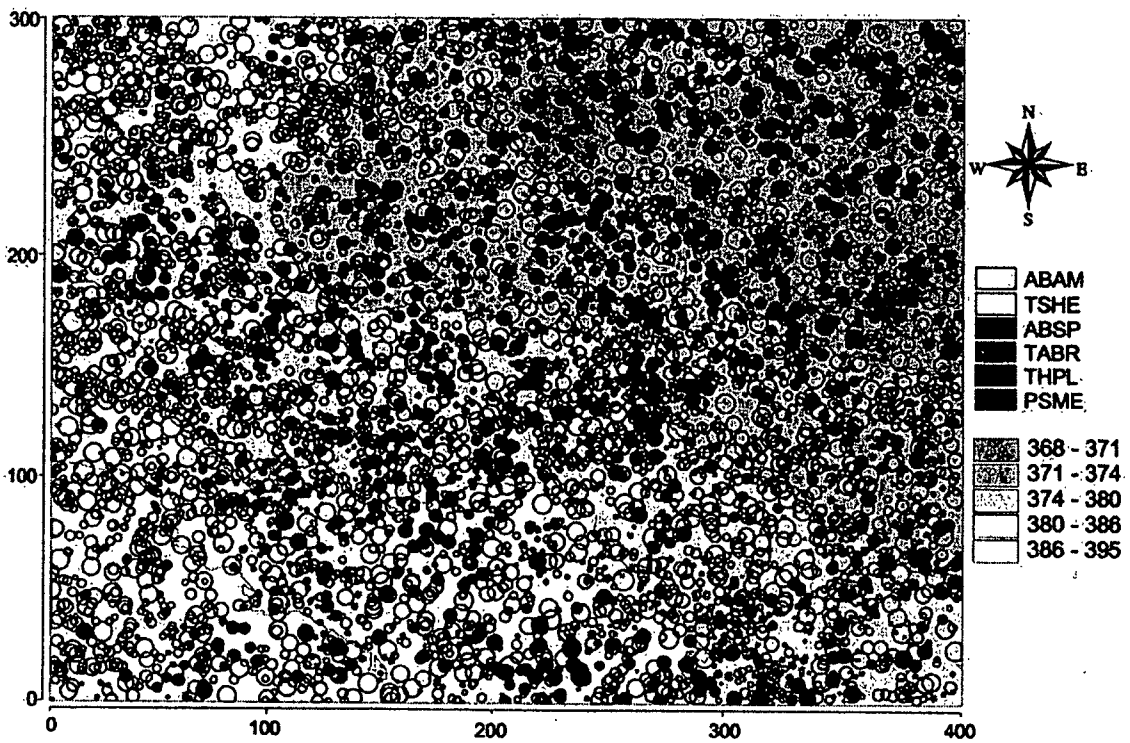

Figure 1. Spatial distribution of tree species on a topographic map in the 12-ha (400 × 300 m) plot facing north. Tree locations and elevations were measured in the summers of 1995, 1996, and 1997 using high accuracy total survey stations within an accuracy of <15 cm. The species and dbh were based on remeasurements in June 1998. The 75-m canopy crane is located at coordinates (300, 200) of the plot.

were calculated based on models for PSME and AGBR, respectively, because of the absence of dbh-height models in the literature. In our first step, using predicted heights and measured dbh, we calculated basal area (BA, m^2) and applied empirical models of Grier and Logan (1977) and Gholz et al. (1979) to calculate foliage biomass (FB, Mg), live branch biomass (Mg), and total stem biomass (Mg) for each tree within the plot. No adjustment was made for wood decay in biomass calculations.

In the second step, a FORTRAN program was developed to simulate randomly located circular plots within the 12-ha plot that sampled the average biomass component of interest on a per hectare basis (e.g., $Mg.ha^{-1}$). In this way, the discrete point patterns of trees were statistically transformed to continuous variables. The program was developed to allow for a variable plot size and number of samples. Our preliminary analysis of comparisons of changes in biomass with plot size and number of samples indicated that a 30-m diameter sample plot, and 500 total sample plots, were sufficient to capture the spatial variability while not being significantly ($P = 0.05$) influenced by the local details. Using these input variables, both the average and number of samples for each of the 500 sample plots as well as plots' coordinates were generated for biomass of each species, FB of all species, total AGB of all species, and BA of individual species as well as that of all the species.

In the third step, we performed semivariance analyses (Cressie 1993) to quantify the spatial autocorrelation of the continuous variables. A maximum lag distance of 150 m (i.e., half of the minimum plot dimension) in 5-m increments was applied in the semivariance analysis. Several variogram models, including exponential, linear, and spherical, were tested to fit changes in semivariance with distance. The spherical models for each variable were presented in this article to allow for consistent comparisons. The values of nugget, sill, range, and correlation coefficient of determination (R^2) of the spherical models (Cressie 1993) were calculated and recorded for further analysis in kriging. One-meter resolution block kriging was performed to emphasize the local variation around the sampling plots. The kriged maps were divided into three zones of biomass: high (4th quartile), medium (2nd and 3rd quartile), and low (1st quartile). For visualizing the spatial patterns of biomass of individual species, five equal bands were used for clear graphical presentations in the illustration. The biomass zones were intersected with the stem-mapped data set to isolate trees falling in each zone. Species composition and density within each biomass zone were calculated using the intersected data to examine the coherent relationships between species distribution and production (e.g., AGB and BA) across the stand.

Results

Forest Structure

The *Pseudotsuga-Tsuga* old-growth forest had an average density of 437 $trees.ha^{-1}$ and an average basal area of 72 $m^2.ha^{-1}$ (Table 1). Diameter frequency distributions for TSHE, ABAM, TABR, and AGBR were skewed toward smaller diameter classes in contrast to PSME (and to some extent THPL), which displayed a more linear distribution (Table 1). Maximum dbh for the above six species ranged from 80 to 187 cm. TSHE and TABR accounted for a total of 77% of the stand density, with TSHE representing over half of the total and TABR another 22%. By BA, TSHE and PSME accounted for 88% of the stand, with TSHE accounting for 44% of the BA. Obvious spatial patterns of tree distribution were visible (Figure 1), with TABR along the ephemeral stream on the north side of the plot, THPL in the northeast quarter of the plot, PSME in the central part of the plot with less PSME in the southwest quadrant, TSHE across the whole plot, and ABAM, AGBR, and ABPR aggregated in several clusters (Figure 1).

Biomass Distribution and Species Composition

Overall, about 86% of the AGB of the major tree species was distributed as stem wood (72%) and branches (14%)

Table 1. Species composition and diameter distribution of an old-growth Douglas-fir forest in the T.T. Munger Research Natural Area, Washington. All live trees greater than 5.0 cm in diameter at breast height (dbh) were stem-mapped and recorded by species and dbh between 1994 and 1999. Stand density (D, $trees.ha^{-1}$) and basal area (BA, $m^2.ha^{-1}$) were calculated using all trees within a 12-ha plot (n = 5,238). Values in the parenthesis indicate species composition (%) of the stand based on D or BA.

dbh class	(cm)	<20	20–40	40–60	60–80	80–100	100–120	120–140	>140	Total
PSME	D			0.66	2.92	8.08	11.08	5.58	2.75	31.08 (7.1)
	BA			0.24	1.14	5.21	10.44	7.24	4.92	29.19 (40.6)
TSHE	D	121.17	50.58	26.33	25.92	15.17	2.42	0.33		241.92 (55.3)
	BA	1.13	3.37	5.14	9.96	9.31	2.12	0.42		31.64 (44.0)
ABAM	D	41.17	4.08	2.08	0.50	0.08				47.92 (11.0)
	BA	0.26	0.26	0.39	0.18	0.04				1.14 (1.6)
THPL	D	3.58	2.08	1.50	2.08	1.58	1.17	1.25	0.83	14.08 (3.2)
	BA	0.04	0.15	0.32	0.86	1.04	1.09	1.61	1.75	6.85 (9.5)
TABR	D	82.50	13.50	1.00	0.08	0.08				96.4 (22.1)
	BA	0.95	0.73	0.16	0.03	0.05				1.92 (2.7)
ABGR	D	0.67	1.17	1.75	0.33	0.17				4.08 (0.9)
	BA	0.01	0.10	0.35	0.12	0.09				0.67 (0.9)
Other	D		0.25	0.08	0.33	0.25	0.25			1.17 (0.3)
	BA		0.02	0.02	0.12	0.14	0.23			0.53 (0.7)
All	D	249.17	71.75	33.33	32.17	25.42	14.92	7.17	3.58	437.5 (100)
	BA	2.70	4.64	6.50	12.41	15.87	13.88	9.27	6.67	71.93 (100)

Table 2. Distribution of aboveground biomass (AGB, Mg.ha^{-1}) among six major tree species and biomass components in a 12-ha plot. Values in the upper parentheses are the proportion of biomass (%) for the species; the lower parentheses give the proportion of biomass (%) of all species for the tree component.

Species	Stem bark	Stem wood	Live branch	Foliage	Total
TSHE	22.919 (7.31)	217.178 (69.26)	62.459 (19.92)	11.035 (3.52)	313.592 (100)
	(31.08)	(45.13)	(69.36)	(58.48)	(47.23)
PSME	46.612 (16.12)	217.430 (75.21)	19.669 (6.80)	5.375 (1.86)	289.086 (100)
	(63.21)	(45.18)	(21.84)	(28.49)	(43.54)
ABAM	0.613 (9.35)	4.877 (74.48)	0.753 (11.51)	0.304 (4.65)	6.654 (100)
	(0.83)	(1.01)	(0.84)	(1.61)	(0.99)
THPL	1.759 (4.93)	28.063 (78.74)	4.558 (12.79)	1.262 (3.54)	35.641 (100)
	(2.38)	(5.83)	(5.06)	(6.69)	(5.37)
TABR	0.682 (7.52)	6.139 (67.73)	1.662 (18.34)	0.581 (6.41)	9.064 (100)
	(0.92)	(1.28)	(1.85)	(3.08)	(1.37)
Other	1.158 (11.56)	7.593 (75.82)	0.950 (9.48)	0.313 (3.13)	10.014 (100)
	(1.57)	(1.58)	(1.05)	(1.66)	(1.51)
Total	73.741 (11.11)	481.279 (72.49)	90.051 (13.56)	18.870 (2.84)	663.944 (100)
	(100)	(100)	(100)	(100)	(100)

(Table 2). A relatively higher percentage of bark biomass was found for PSME (16%) compared with other species (Table 2). The average AGB (664 Mg.ha^{-1}) was dominated by TSHE (47%) and PSME (44%), with THPL being the next highest contributor (5%). In addition to their spatially aggregated characteristics, the biomass distributions of all six major tree species were spatially heterogeneous based on higher R^2 values and relatively low nugget effects in semivariance analysis (Figure 2). PSME had a maximum biomass patch size (i.e., range value) of 115 m, while AGBR and THPL had smaller patch sizes (37 and 39 m, respectively, Figure 2). The highest nugget effect (i.e., indicating high local variation) was found for ABAM (25%)—a species showing the strongest clustering pattern in the plot (Figure 3). Distinct biomass patches existed for all six species (Figure 3), with TSHE biomass negatively correlated with low elevations (Figure 3a and Figure 1) and TABR positively correlated with the ephemeral stream (Figure 3f and Figure 1). THPL biomass was highly aggregated in the northeast quadrant of the plot (Figure 3e); and the biomass of *Abies* species was clustered in several isolated patches (Figure 3, b and c).

Relatively low nugget (6.5–12.6%) and high R^2 (89.4–85.6%) values were calculated in semivariance analysis for three biomass measurements: BA, AGB, and FB (Figure 4), suggesting strong patch-patterns and variation for these variables across the stand (Figure 5). The average patch sizes (i.e., range value) for BA, AGB, and FB were 46.5, 41.1, and 32.5 m, respectively (Figure 4, a–c). Kriged contour distributions of these variables (Figure 5) suggested distinct low and high biomass islands across the stands. The high/low islands of BA, AGB, and FB showed some positive spatial correlation with each other. High biomass zones tended to be distributed at lower elevations around the ephemeral stream, while low biomass islands were distributed at higher elevations in the plot (Figure 5).

Several compositional characteristics were related to the distribution of biomass zones in the plot. First, high biomass zones had higher proportions of PSME and THPL, but lower proportions of TSHE and ABAM in both AGB and density (Figure 6). Likewise, low biomass zones were characterized by higher proportions of TSHE and ABAM. TABR biomass was higher in low biomass zones but its density was close to the stand average, suggesting that there are larger TABR trees in the low biomass zones. The biomass and density composition of medium biomass zones of the plot were not always similar to stand average values. These zones had relatively low PSME, THPL, and TABR biomass and density, but higher TSHE and ABAM proportions.

The biomass levels across the stand were also related to the biomass and density of different dbh classes (Tables 3 and 4). The high biomass zones had more PSME trees in all dbh classes, TABR in smaller dbh classes, and THPL in dbh classes larger than 60 cm; and fewer numbers of TSHE and ABAM in all dbh classes (Table 3). Similarly, low biomass zones had higher density of TSHE in smaller dbh classes (<60 cm) but relatively low density of larger TSHE in dbh classes greater than 60 cm. These low biomass zones had more small dbh ABAM trees. Stand density of TABR trees was significantly higher in all dbh classes in the low biomass zones.

Finally within the stand, biomass zones were formed depending on tree size distribution and species composition (Table 4). For the high biomass zones, there was higher biomass of PSME in all dbh classes and higher THPL biomass in larger dbh classes (>60 cm); but TSHE contributes consistently less in all dbh classes. Medium biomass zones were predominantly characterized by significantly higher proportions of TSHE between 60 and 100 cm in dbh. Based on all species pooled by diameter class, high biomass zones had more biomass from trees >80 cm and lower biomass component from trees < 80 cm. The low biomass zone had higher proportion of biomass contributed by trees <60 cm than did the medium biomass zone.

Discussion

The biomass distribution of individual species and all species support the idea that spatial patterns need to be explored at various scales (Figure 3 and 5). The patch

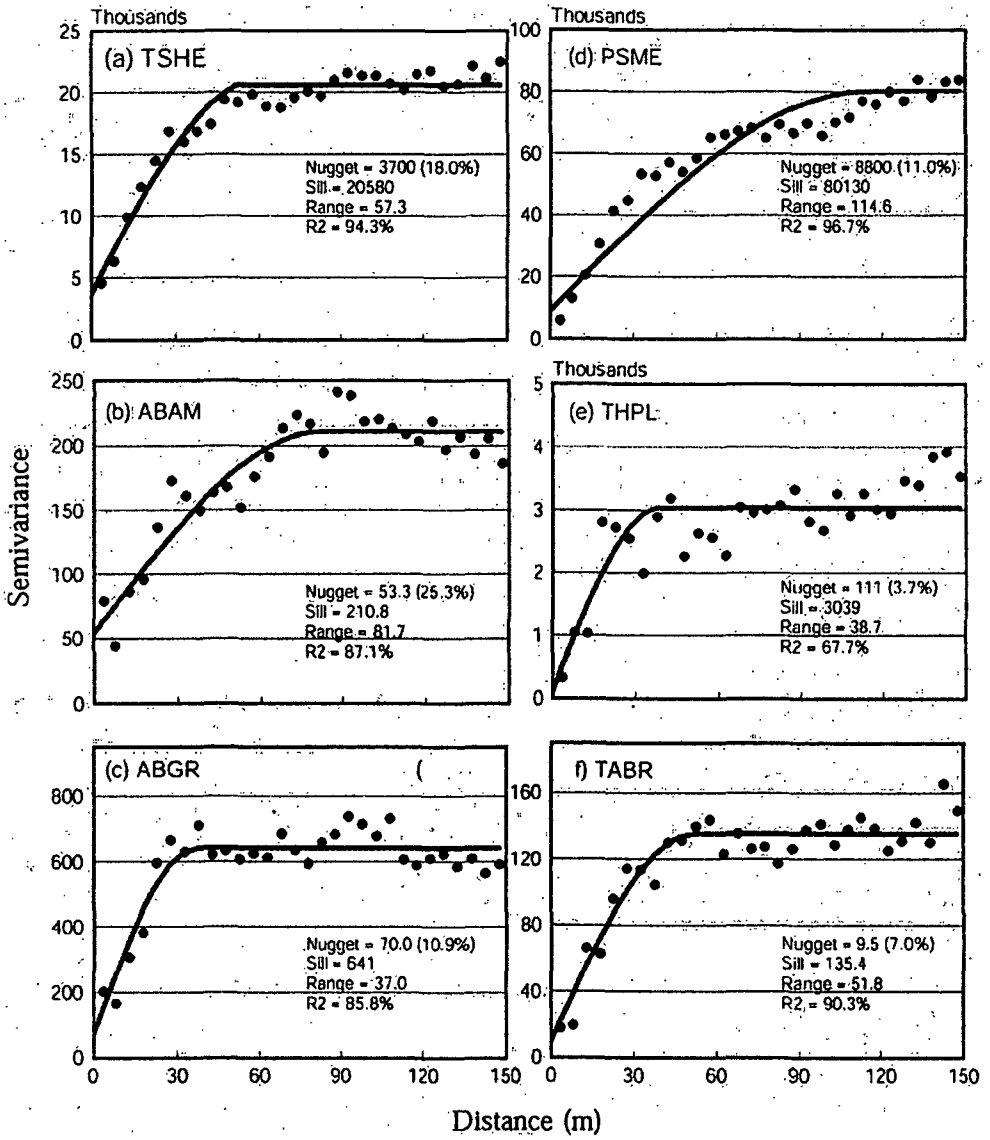

Figure 2. Semivariances of basal area (a), aboveground biomass (b), and foliage biomass (c) for distance up to half of the minimum plot dimension (i.e., 150 m). Five hundred 30-m diameter simulated circular sampling plots were randomly placed within the 12-ha plot to convert the point pattern to a continuous variable on a per hectare basis. Spherical models were used to calculate the range, sill, nugget, and R^2 values.

pattern of biomass of AGBR and THPL were repeated at scales between 37 and 38.5 m (Figure 2, c and e), suggesting a minimum plot size of 40 m needed for adequate estimations of their contribution to the total biomass. However, for ABAM and PSME, their average patch size was 82 and 114 m, respectively (Figure 2, b and d). Clearly, both structure and function of the forest ought to be explored at appropriate scales (Holling 1992) and across a range of scales (Levin 1992). With the above conclusion, we argue that results based on fixed plot size less than 100 m would be very questionable.

The spatial distribution of species and their spatial associations reflected the spatial pattern of biomass (Figure 5). After we converted the discrete stem data to continuous variables of biomass and basal area, geostatistical tools were applied to detect the patchiness of each variable across the stand. Applications of such an approach are not error-free. First, the number and size of sampling plot need to be carefully examined because the means generated based on the above averages will have profound effects on semivariance analysis. Second, semivariance analysis does not help us to reveal underline patterns at multiple scales (Bradshaw and Spies 1992, Cressie 1993). Nevertheless, the formation of biomass patches based on semivariance analysis in this study appeared complex, especially when generating a spatial biomass patterns based on patch pattern of individual species. Each species had a unique biomass patch pattern such as size, shape, and spatial distribution (Figures 2 and

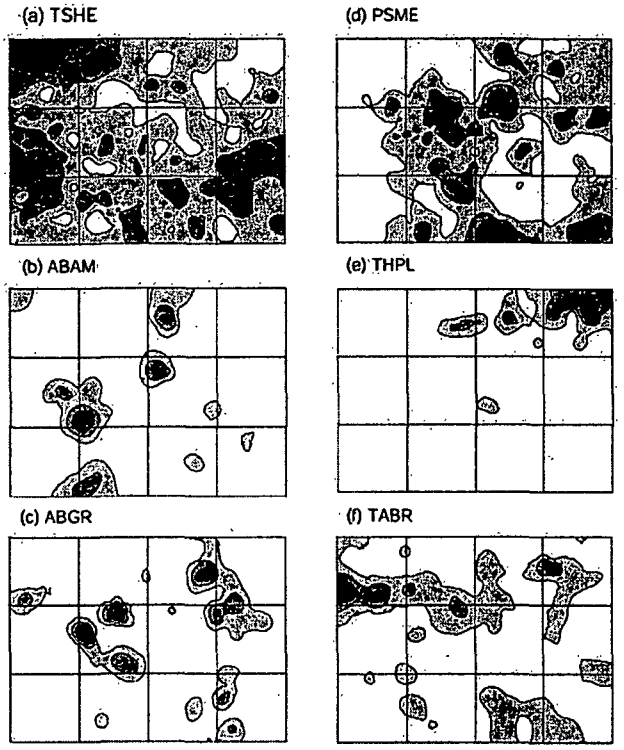

Figure 3. Spatial distribution of aboveground biomass (AGB) for the six major species in a 12-ha old-growth Douglas-fir forest in southern Washington. The five contour lines represent an equal division from the minimum to the maximum value. Kriging predictions were made using the spherical models in Figure 5 at 1-m resolution.

3). From Figure 3, it is clear that the spatial patterns of different species were mostly repulsive, with occasional overlaps. While each patch pattern contributed a different proportion to the overall biomass mosaic, the nonperfect exclusivity of patch patterns of the six species were probably responsible for the reduction in the scale of interaction of all three biomass measurements: BA, AGB, and FB, which ranged between 32 and 46 m (Figure 4). For example, high biomass patch H1 was formed because of high PSME biomass and intermediate TSHE biomass (Figure 3, a and d), while another high biomass patch H2 (Figure 5b) was likely associated with the high proportion of THPL (Figure 3e) and the absence of TSHE (Figure 3a). In both cases, patch size was reduced because of nonperfect exclusivity of multiple patterns in space.

An interesting result of this study was the high variation in biomass distribution across the stand and the distinct species composition for high-to-low biomass zones. The ecological literature suggests that old-growth Douglas-fir forests have high biomass ranging from 800 to 1600 $Mg.ha^{-1}$ depending on stand location in the larger landscape (e.g., Franklin et al. 1981). The stand biomass of our stand was reported as 830 $Mg.ha^{-1}$ (see Parker et al., in press). In contrast, the stem map depicts a forest that was not homogeneous, with biomass ranging from 0 to 1600 $Mg.ha^{-1}$ (Franklin and Waring 1980). TSHE and/or PSME and

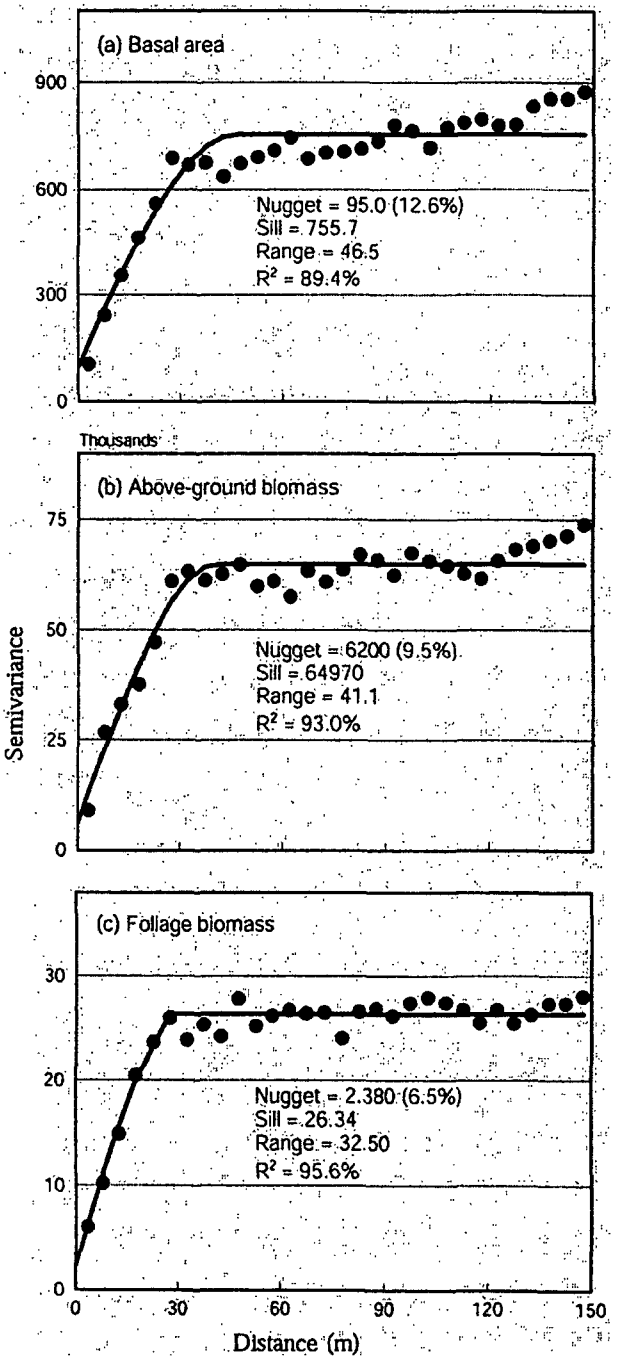

Figure 4. Changes in semivariances of the aboveground biomass for distance up to half of the minimum plot dimension (i.e., 150 m) for the six major species in a 12-ha plot. Five hundred 30-m diameter simulated circular sampling plots were randomly placed within the plot to convert the point pattern to a continuous variables on a per hectare basis. Spherical models were used to calculate the range, sill, nugget, and R^2 values.

THPL dominated the high biomass zones, with little overlap between them because the two species showed a clearly repulsive relationship, and low-biomass zones were dominated by mixtures of shade-tolerant species such as TABR and ABAM (Figure 6). These findings were in agreement with other studies (Franklin and Waring 1980, Franklin et

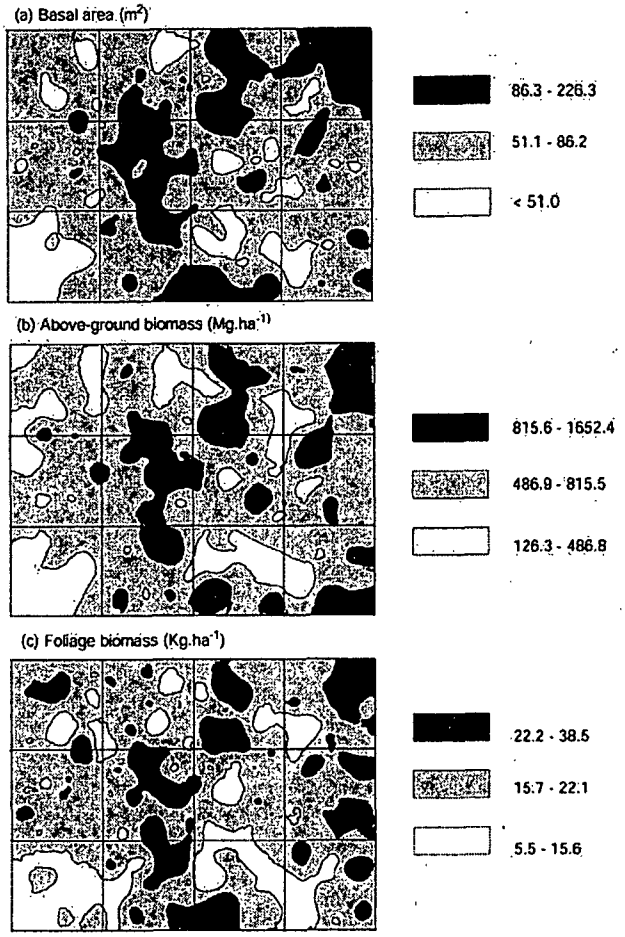

Figure 5. Spatial distribution of low (1st quartile), medium (2nd and 3rd quartiles), and high (4th quartile) of basal area (a), aboveground biomass (b), and foliage biomass (c) in a 12-ha old-growth Douglas-fir forest in southern Washington. Kriging predictions were made using the spherical models at 1-m resolution.

al. 1981) that suggested high biomass stands in broader landscapes in the Pacific Northwest were results of high proportion of PSME and THPL. It appeared that biomass-species relationships for the Douglas-fir forests may hold at any scale ranging from the patch to the landscape. PSME and THPL are long-lived species but will gradually decline relative to TSHE and *Abies* in the forest over the next 500 years. Due to the close spatial relationships between species composition and biomass, we would expect not only that stand biomass will decrease, but also that a new biomass mosaic will emerge.

The spatial distribution of trees, canopy patch patterns, and the relationship among these distributions and patchiness of biomass in this old-growth forest was a product of multiple ecological processes over a span of at least 500 years (Franklin et al. 2002). As pioneer ecologist Ramon Margalef stated, "Structure, in general, becomes complex, more rich, as time passes; structure is linked to history" (Margalef 1963). To understand patterns presented in this study requires careful exploration of various processes, including their frequency, intensity, and duration in the past five centuries. Although the underlying mechanisms responsible for these patterns and associations cannot be identified in detail with our field data, it was apparent that multiple mechanisms control spatial pattern and dynamics of a forest.

Stand structure and composition in an old-growth forest are usually viewed as the current manifestation of ongoing successional processes. During the time between stand replacement disturbances, *Pseudotsuga-Tsuga* forest stand dynamics are often modeled as gap-phase replacement (Spies and Franklin 1989, Lertzmann et al. 1996). Stand dynamics theory in silviculture also suggests that old-growth forests undergo slow replacement of pioneer species until a stand-replacement disturbance occurs (Oliver and Larson 1990). In studying old-growth eastern hemlock (*Tsuga canadensis* (L.) Carr.) in the upper Midwest, Frelich et al. (1993) proposed four hypotheses to explain the current old-growth conditions: soil and topographic variation, disturbance history, competitive interactions among trees, and invasive patterns. We believe at least four additional factors should be considered: (1) size and reproductive characteristics of the tree species such as their maximum tree height and age, seed production cycle and establishment, growth, and mortality, (2) ecology of tree species such as species responses and habitat requirements for light, moisture, and disturbances, (3) stand dynamics such as species replacement during forest succession, and (4) the random nature of many processes in time and space.

The biology of tree species in a forest is the basic information needed to understand some aspects of spatial patterns because each species has a unique form (roots, stems, and crowns), size, longevity, seed production cycle, rooting structure, and phenology. These evolutionary attributes directly control some aspects of spatial pattern and indirectly affect processes responding to disturbances and competition (Peet and Christensen 1987, White et al. 1999, Parker et al. in press). Most forests other than plantations are composed of more than one tree species with each species having a unique spatial pattern at any successional stage. In a detailed examination of species distribution in a tropical rainforest in Malaysia, He et al. (1997) found that 80% of 745 species were clustered while others were randomly distributed. No regular distribution was found for any species. Depending on the situation and level of aggregation for each species, very complex (but unique) patches can form, which in turn may be partially responsible for high functional variability across a tropical forest (cf. He et al. 1997). Even in a low diversity stand of southern boreal forest where three species (*Picea*, *Abies*, and *Betula*) dominate the forest, Chen and Bradshaw (1999) found that very complex patches were formed with different portions and distributions of various-sized individuals. These studies suggested the need to examine the spatial arrangement of individual species, emphasizing the spatial relationships among species in three-dimensional space and time (i.e., across succesional stages, Van Pelt and Nadkarni 2004) and their potential roles in determining ecosystem function such

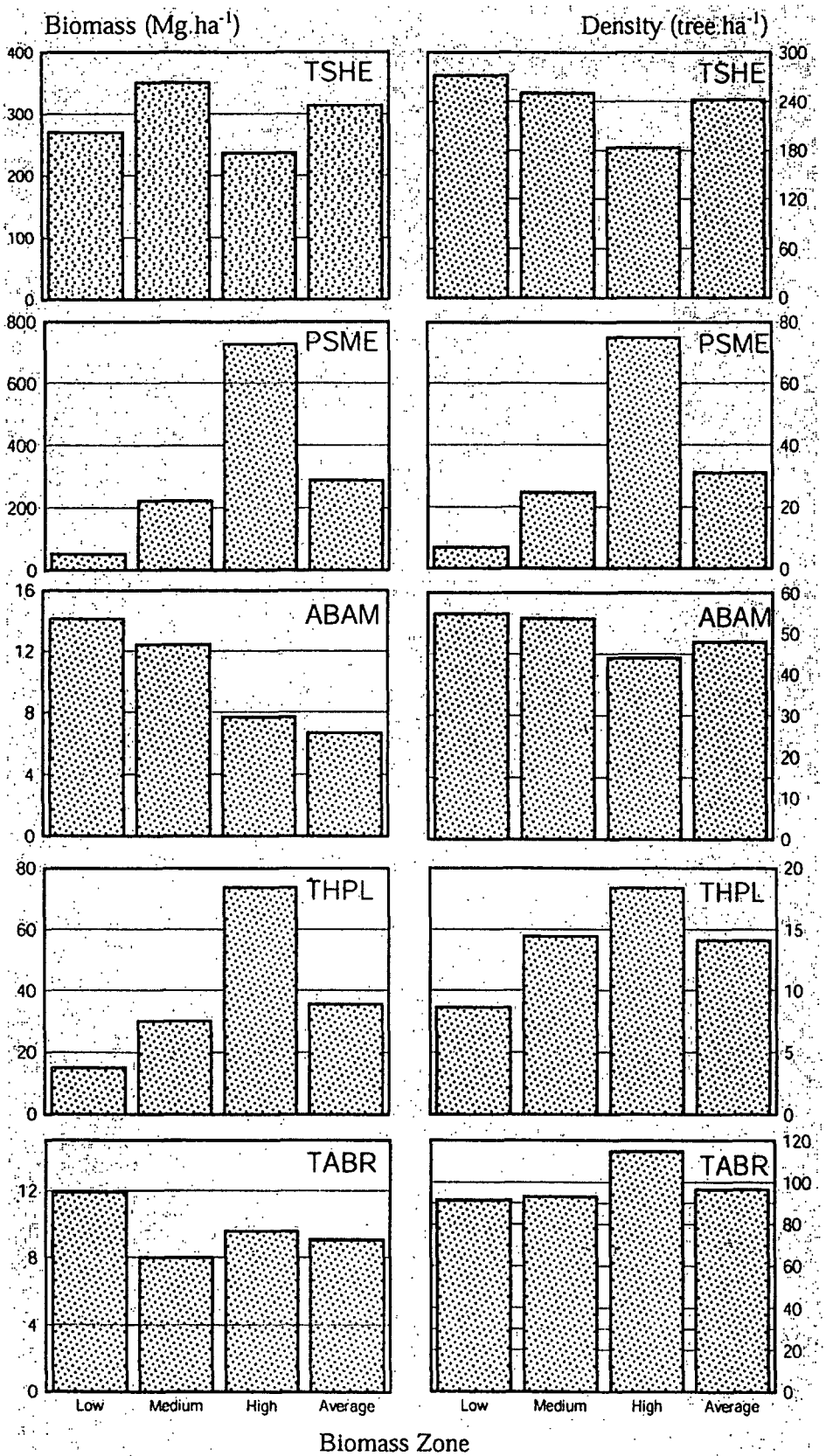

Figure 6. Stand biomass and density of five major species (i.e., ABAM and AGBR combined because of low AGBR component) in low, medium, and high biomass zones of the 12-ha plot.

Table 3. Biomass distribution of five dominant tree species in low (1st quartile, 126.3–486.8 Mg.ha^{-1}), medium (2nd and 3rd quartile, 486.7–815.5 Mg.ha^{-1}), and high (4th quartile, 815.6–1,652.4 Mg.ha^{-1}) biomass zone in the 12-ha plot. See Figure 6b for spatial patterns of the biomass zones as defined in the methods.

dbh class (cm)	Biomass zone	Biomass by species (Mg.ha^{-1})					
		PSME	TSHE	ABAM	THPL	TABR	Total
<20	Low	4.23		0.49	0.02	3.56	8.30
	Medium	3.72		0.55	0.05	3.49	7.81
	High	2.61		0.91	0.07	4.92	8.51
20–40	Low	19.41		2.28	0.34	5.37	27.40
	Medium	19.81		1.85	0.42	2.98	25.06
	High	18.61		5.02	0.16	4.33	28.12
40–60	Low	57.03	0.93	3.05	0.37	1.80	63.18
	Medium	44.39	0.28	6.44	1.36	0.92	53.39
	High	30.52	1.94	1.78	0.91	0.32	35.47
60–80	Low	85.64	4.71	4.12	2.61	1.17	98.25
	Medium	116.89	8.93	2.90	2.98		131.70
	High	85.95	15.75		6.32		108.02
80–100	Low	89.11	8.22	4.18	3.06	0.60	104.57
	Medium	126.80	41.30	0.67	6.21		175.58
	High	71.48	109.73		2.75		183.96
100–120	Low	14.26	24.51		2.37		41.14
	Medium	32.73	78.13		4.03		82.16
	High		259.81		14.15		307.05
120–140	Low	19.47	6.54		6.20		32.21
	Medium	6.48	58.56		7.08		72.12
	High	8.26	191.10		18.11		217.47
>140	Low		7.41		7.91		7.41
	Medium		34.66		31.27		42.57
	High		150.14				181.41

Table 4. Frequency distribution of five major tree species by their dbh class in low (1st quartile, 126.3–486.8 Mg.ha^{-1}), medium (2nd and 3rd quartile, 486.7–815.5 Mg.ha^{-1}), and high (4th quartile, 815.6–1,652.4 Mg.ha^{-1}) biomass zones in the 12-ha plot. See Figure 5b for spatial patterns of the biomass zones.

dbh class (cm)	Biomass zone	Stand density by species (trees.ha^{-1})					
		PSME	TSHE	ABAM	THPL	TABR	Total
<20	Low		154.81	44.42	2.16	71.15	272.54
	Medium		120.77	42.89	3.95	80.74	248.35
	High		87.73	36.80	3.85	98.43	226.81
20–40	Low		154.81	6.04	1.72	18.11	74.16
	Medium		120.77	5.17	2.59	11.44	72.44
	High		87.73	3.85	0.86	15.83	64.62
40–60	Low	0.86	34.01	2.16	0.86	1.72	39.61
	Medium	0.27	26.42	4.49	1.77	0.95	33.90
	High	1.28	18.40	1.28	1.28	0.43	22.67
60–80	Low	1.29	21.13	1.29	1.72	0.43	25.86
	Medium	2.72	29.00	0.95	1.63		34.30
	High	5.14	20.97	2.14	3.85		32.10
80–100	Low	1.29	12.07	0.86	0.86	0.14	15.08
	Medium	6.94	17.70	0.14	2.04		26.96
	High	18.40	9.84		0.86		29.10
100–120	Low	2.59	1.29		0.43		4.31
	Medium	8.44	3.00		0.82		12.26
	High	27.82	1.71		3.00		32.53
120–140	Low	0.43	0.41		0.86		1.70
	Medium	4.36	0.43		0.95		5.31
	High	14.55			2.57		17.55
>140	Low	0.43			0.68		0.43
	Medium	1.91			2.14		2.59
	High	7.70					9.84

as productivity and, ultimately, spatial distribution of biomass across the stand.

Patch patterns and their cohesive spatial relationships are scale-dependent, spatially and temporally. While shade-tolerant species tend to aggregate at smaller scales, larger PSME trees exhibit an average patch size of 114 m (North

et al. 2004), suggesting that a plot containing at least 100 canopy patches (i.e., gaps) is necessary to fully sample the configuration of overall forest structure. Specific species composition is responsible for the level and mosaic of biomass patches observed in the present day forest. Clearly, further studies are needed to reveal the details of how each process alters the spatial patterns of tree species with a complete factorial experimental design, and long-term monitoring process at broader scales is needed. An alternative is to examine the current spatial patterns and relate their spatial information to the possible underlying mechanisms and processes.

Literature Cited

BOTKIN, D.B. 1993. Forest dynamics: An ecological model. Oxford University Press, New York, NY. 309 p.

BRADSHAW, G.A., AND T.A. SPIES. 1992. Characterizing canopy gap structure in forests using the wavelet transform. J. Ecol. 80:205–215.

BURKE, I.C., W.K. LAUENROTH, R. RIGGLE, P. BRANNEN, B. MADIGAN, AND S. BEARD. 1999. Spatial variability of soil properties in the shortgrass steppe: The relative importance of topography, grazing, microsite, and plant species in controlling spatial patterns. Ecosystems 2:422–438.

BUSING, R.T. 1998. Composition, structure and diversity of cove forest stands in the Great Smoky Mountains: A patch dynamics perspective. J. Veg. Sci. 9:881–890.

CHEN, J., AND G.A. BRADSHAW. 1999. Forest structure in space: A case study of an old growth spruce fir forest in Changbaishan Natural Reserve, PR China. For. Ecol. Manage. 120:219–233.

CHEN, J., AND J.F. FRANKLIN. 1997. Growing-season microclimate variability within an old-growth Douglas-fir forest. Clim. Res. 8(1):27–34.

CHEN, J., S.D. SAUNDERS, T. CROW, K.D. BROSOFSKE, G. MROZ, R. NAIMAN, B. BROOKSHIRE, AND J. FRANKLIN. 1999. Microclimatic perspectives in forest ecosystems and landscapes. BioScience 49(4):288–297.

CRESSIE, N.A. 1993. Statistics for spatial data. John Wiley & Sons, New York, NY. 900 p.

DEBELL, D.S., AND J.F. FRANKLIN. 1987. Old-growth Douglas-fir and western hemlock: A 36-year record of growth and mortality. West. J. Appl. For. 2:111–114.

FRANKLIN, J.F, K. CROMACK, JR., W. DENISON, A. MCKEE, C. MASER, J. SEDELL, F. SWANSON, AND G. JUDAY. 1981. Ecological characteristics of old-growth Douglas-fir forest. USDA For. Serv. Gen. Tech. Rep. PNW-118. Portland, OR. 48 p.

FRANKLIN, J.F., AND D.S. DEBELL. 1988. Thirty-six years of population change in an old-growth *Pseudotsuga-Tsuga* forest. Can. J. For. Res. 18:633–639.

FRANKLIN, J.F., T.A. SPIES, R. VAN PELT, A.B. CAREY, D.A. THORNBURGH, D.R. BERG, D.B. LINDENMAYER, M.E. HARMON, W.S. KEETON, D.C. SHAW, K. BIBLE, AND J. CHEN. 2002. Disturbances and structural development of natural forest ecosystems with silvicultural implications, using Douglas-fir forests as an example. For. Ecol. Manage. 155:399–423.

FRANKLIN, J.F., AND R.H. WARING. 1980. Distinctive features of the northwestern coniferous forest: Development, structure, and function. P. 59–85 *in* Ecosystem analysis: Proc. 40th Ann. Biol. Colloquium, 1979 April 27–28, Corvallis, OR.

FREEMAN, L. 1997. The effects of data quality on spatial statistics. M.S. thesis, Univ. of Wash. 111 p.

FRELICH, L.E., R.R. CALCOTE, M.B. DAVIS, AND J. PASTOR. 1993. Patch formation and maintenance in an old-growth hemlock-hardwood forest. Ecology 74:513–527.

GHOLZ, H.L., C.C. GRIER, A.G. CAMPBELL, AND A.T. BROWN. 1979. Equations for estimating biomass and leaf area of plants in the Pacific Northwest. Oregon State University, Forest Research Laboratory, Res. Pap. 21, Corvallis, OR. 39 p.

GRAY, A.N., AND T.A. SPIES. 1997. Microsite controls on tree seedling establishment in conifer forest canopy gaps. Ecology 78:2458–2473.

GRIER, C.C., AND R.S. LOGAN. 1977. Old-growth *Pseudotsuga menziesii* communities of a western Oregon watershed: Biomass distribution and production budgets. Ecol. Monogr. 47:373–400.

HE, F., P. LEGENDRE, AND J.V. LAFRANKIE. 1997. Distribution patterns of tree species in a Malaysian tropical rain forest. J. Veg. Sci. 8:105–114.

HOLLING, C.S. 1992. Cross-scale morphology, geometry, and dynamics of ecosystems. Ecol. Monogr. 62:447–502.

ISHII, H., J.H. REYNOLDS, E.D. FORD, AND D.C. SHAW. 2000. Height growth and vertical development of an old-growth *Pseudotsuga-Tsuga* forest in southwestern Washington, U.S.A. Can. J. For. Res. 30:17–24.

LERTZMAN, K.P., G.D. SUTHERLAND, A. INSELBERG, AND S.C. SAUNDERS. 1996. Canopy gaps and the landscape mosaic in a coastal temperate rain forest. Ecology 77:1254–1270.

LEVIN, S.A. 1992. The problem of pattern and scale in ecology. Ecology 73:1943–1967.

LIEBERMAN, K., D. LIEBERMAN, AND R. PERALTA. 1989. Forests are not just Swiss cheese: Canopy stereometry of non-gaps in tropical forests. Ecology 70:550–552.

MARGALEF, R. 1963. On certain unifying principles in ecology. Am. Nat. 897:357–375.

MOEUR, M. 1993. Characterizing spatial patterns of trees using stem-mapped data. For. Sci. 39(4):756–775.

NORTH, M., J. CHEN, B. OAKLEY, B. SONG, M. RUDNICKI, AND A. GRAY. 2004. Forest stand structure and pattern of old-growth western hemlock/Douglas-fir and mixed-conifer forests. For. Sci. 50:299–311.

OLIVER, C.D., AND B.C. LARSON. 1990. Forest stand dynamics. McGraw-Hill, New York, NY. 520 p.

PARKER, G.G., M.E. HARMON, M.A. LEFSKY, J. CHEN, R. VAN PELT, S.B. WEISS, S.C. THOMAS, W.E. WINNER, D.C. SHAW, AND J.F. FRANKLIN. Three-dimensional structure of an old-growth *Pseudotsuga-Tsuga* canopy and its implications for radiation balance, microclimate and gas exchange. Ecosystems, in press.

PEET, R.K., AND N.L. CHRISTENSEN. 1987. Competition and tree death. Bioscience 37:586–595.

PICKETT, S.T.A., AND P.S. WHITE (EDS.). 1985. The ecology of natural disturbance and patch dynamics. Academic Press, New York, NY. 472 p.

RUDNICKI, M., AND J. CHEN. 2000. Relations of climate and radial increment of western hemlock in an old-growth Douglas-fir forest in southern Washington. Northwest Sci. 74(1):57–68.

RUNKLE, J.R. 1981. Gap generation in some old-growth forests of the eastern United States. Ecology 62:1041–1051.

SCHLESINGER, W.H., J.A. RAIKERS, A.E. HARTLEY, AND A.F. CROSS. 1996. On the spatial pattern of soil nutrients in desert ecosystems. Ecology 77:364–374.

SONG, B. 1998. Three-dimensional forest canopies and their spatial relationships to understory vegetation. Ph.D. dissertation, Michigan Tech. Univ., Houghton, MI, 160 p.

SONG, B., J. CHEN, P.V. DESANKER, D.D. REED, G.A. BRADSHAW, AND J.F. FRANKLIN. 1997. Modeling canopy structure and heterogeneity across scales: From crowns to canopy. For. Ecol. Manage. 96:217–229.

SPIES, T.A., AND J.F. FRANKLIN. 1989. Gap characteristics and vegetation response in tall coniferous forests. Ecology 70:543–545.

SZWAGRZYK, J. 1990. Small-scale spatial patterns of trees in a mixed *Pinus sylvestris-Fagus sylvatica* forest. For. Ecol. Manage. 51:301–315.

VAN PELT, R., AND J.F. FRANKLIN. 1999. Response of understory trees to experimental gaps in old-growth Douglas-fir forests. Ecol. Applic. 9:504–512.

VAN PELT, R., AND N.M. NADKARNI. 2004. Changes in the vertical and horizontal distribution of canopy structural elements in an age sequence of *Pseudotsuga menziesii* forests in the Pacific Northwest. For. Sci. 50:326–341.

WARD, J.S., G.R. PARKER, AND F.J. FERRANDINO. 1996. Long-term spatial dynamics in an old-growth deciduous forest. For. Ecol. Manage. 83:189–202.

WHITE, P.S., J. HARROD, W.H. ROMME, AND J. BETANCOUT. 1999. Disturbance and temporal dynamics. P. 281–312 *in* Ecological stewardship: A common reference for ecosystem management, Johnson, N.C., A.J. Malk, R.C. Szaro, and W.T. Sexton (eds.). Elsevier Science Ltd., Sexton, NY. 305 p.